Available online at www.sciencedirect.com
SCIENCE DIRECT®
Composite Structures 63 (2004) 375–385
COMPOSITE STRUCTURES
www.elsevier.com/locate/compstruct

The elastic response of sandwich structures to local loading

Vitaly Koissin [a,*], Vitaly Skvortsov [b], Sergey Krahmalev [b], Andrey Shilpsha [a]

[a] Department of Aeronautical and Vehicle Engineering, Royal Institute of Technology, S-100 44, Stockholm, Sweden
[b] Department of Strength of Materials, State Marine Technical University, 198 262 St. Petersburg, Russia

Abstract

The paper addresses the elastic response of sandwich panels to local static and dynamic loading. The bottom face is assumed to be clamped, so that the overall bending is eliminated. The governing equations are derived using the static Lamé equations for the core and the thin plate Kirchoff–Love dynamic theory for the faces. The plane and axisymmetric formulations are considered. The closed-form solutions are obtained using Fourier–Laplace (Hankel–Laplace) integral transformations for the cases of forced excitation and impact by a rigid body. The solutions allow to predict the stress–strain state of the structure. The analytical solutions demonstrate a good agreement with experimental data and finite element analysis.

Keywords: Sandwich plate; Concentrated forced excitation; Impact; Local stress

1. Introduction

One of the inherent properties of sandwich structures is low transversal stiffness, causing local bending under concentrated loads. As a result, these structures are susceptible to local damages due to handling, interaction with attached structures or impact. Usually, the local failure starts in the core and results in core crushing, face–core debonding and (or) residual dent formation and, therefore, in substantial reduction of the structural strength [1]. Thus, it is of a practical importance to predict the elastic stress–strain response of sandwich structures subject to localized loads.

Besides experimental and finite element analysis, e.g. [1–4], there are two approaches to analytical modelling of sandwich structure local behaviour. These approaches are based on different descriptions of core deformation.

The simplified approach is based on the assumption that the plate is resting on a continuously distributed set of independent springs, the stiffness of which defines the Winkler foundation modulus and results in dependence of the interface stress only on the deflection at the same point. The main problem of this approach concerns determination of the modulus using characteristics of the sandwich layers. A complete correspondence between the Winkler type foundation and a elastic layer can be found only for a thin core; in this case the modulus can be obtained solely. For the case of a thick core determination of the modulus can be fulfilled by various means (for instance, to ensure coincidence of deflection, bending moments or interface stress under a concentrated force in exact and simplified formulations). These two limit cases (very thin and very thick core) are used for solving numerous static problems in [3–7]. Dynamic analysis for the given modulus is performed in [8,9]. In many cases the Winkler model or the more advanced Winkler–Pasternak model [3,4,10] provides satisfactory agreement with experimental results, but it is not universal for a general case of the sandwich constitution.

The more precise approach is based on the elastic continuum model that results in interconnectivity of strain–stress state at all points of an interface. Applying the linear theory of elasticity, static behaviour of a plate resting on the elastic core layer under arbitrary load was analyzed in [11–13], simplified solutions are given in [14], implementation to the problems of stability is discussed in [15]. All these results are generalizations of the well-known solutions for a semi-infinite medium that models a thick core [16,17]. Dynamic analysis of the single elastic layer (Lamb's problem) was performed in [18,19]. Stationary oscillations of a face sheet resting on an elastic layer are considered in [8,20].

* Corresponding author. Fax: +48-8-20-78-65.
E-mail address: vitaly@kth.se (V. Koissin).

0263-8223/$ - see front matter © 2003 Elsevier Ltd. All rights reserved.
doi:10.1016/S0263-8223(03)00186-7

In the present paper, the elastic continuum model is successfully used for the analysis of non-stationary oscillations of a locally loaded sandwich panels of arbitrary thickness. The case of static loading is considered as a supplement for the analysis of dynamic loading. The closed-form solutions are obtained for the particular cases of static and dynamic forced excitation and impact by a rigid body. A comparison of the analytical results with numerical solutions and experimental data demonstrates a good agreement.

1.1. Notations

Subscript "f" belongs to the face, "c" --- to the core, "if" --- to the face–core interface. Superscripts "F", "H" and "L" belong to the Fourier, Hankel and Laplace transforms, respectively, "pl" --- to the plane formulation and "ax" --- to the axisymmetrical formulation. Subscript "0" means that a function is examined at the co-ordinate origin.

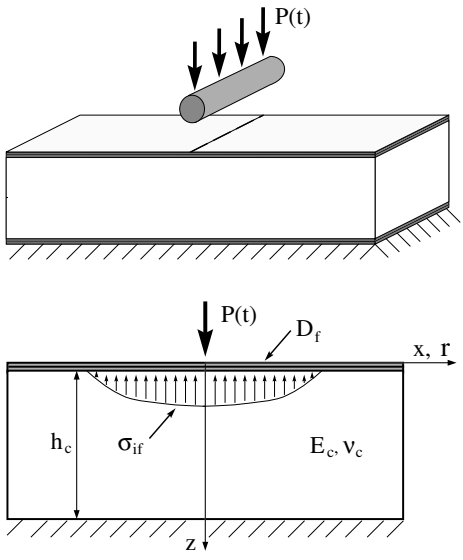

Fig. 1. Impact set-up for plane formulation (top) and physical model (bottom).

2. Analytical modelling

A three-layered sandwich panel is studied under a point or line load. No overall bending is considered. The panel consists of two thin and stiff face sheets with thickness h_f and relatively thick and light-weight core with thickness h_c. The densities of the face and the core are ρ_f and ρ_c, respectively.

The local bending of the top face is considered in the plane (plane stress and plane strain) and axisymmetric formulations. The face is modelled as in-plane isotropic, infinite plate with bending stiffness D_f bonded to the core layer (Fig. 1). The plate is assumed to be thin and non-stretchable. Thus, no difference is assumed between displacements of the midplane and the interface and no influence of the shear stresses on bending of the plate. Under these assumptions, the thin plate Kirchoff–Love dynamic theory is used for the face bending under external excitation $P(t)$ and normal core reaction σ_{if}, see Fig. 1. For the plane formulation, the governing equation for the face deflection w_f is

$$D_f \frac{\partial^4 w_f(x,t)}{\partial x^4} + \rho_f h_f \frac{\partial^2 w_f(x,t)}{\partial t^2} = \frac{\delta(x)}{2b} P(t) - \sigma_{if}(x,t), \quad (1)$$

where δ is the delta-function, b is the width of the beam, and for the axisymmetric formulation is

$$D_f \Delta\Delta w_f(r,t) + \rho_f h_f \frac{\partial^2 w_f(r,t)}{\partial t^2} = \frac{\delta(r)}{2\pi r} P(t) - \sigma_{if}(r,t),$$
$$\Delta = \frac{\partial^2}{\partial r^2} + \frac{\partial}{r\partial r}. \quad (2)$$

Since ρ_c is small, the core inertia is neglected and the core behaviour is described by the static Lamé equations for isotropic elastic continuum. The Lamé equations are solved by means of Fourier or Hankel integral transformation technique. For symmetric functions (e.g. deflection and normal interfacial stress), the cosine Fourier transformation is used in the plane formulation

$$w_f^F(\omega) = \int_0^\infty w_f(x)\cos(\omega x)\,dx,$$
$$w_f(x) = \frac{2}{\pi}\int_0^\infty w_f^F(\omega)\cos(\omega x)\,d\omega$$

and zero-order Hankel transformation is used in the axisymmetric problem

$$w_f^H(\omega) = \int_0^\infty w_f(r) J_0(\omega r) r\,dr,$$
$$w_f(r) = \int_0^\infty w_f^H(\omega) J_0(\omega r)\omega\,d\omega.$$

Analogously, the sine Fourier or first-order Hankel transformation is used for the other functions (rotation, shear stress etc.). The integral transformation technique is discussed in detail in [13,18,19].

The transformations for the Lamé equations are performed under the boundary conditions of zero longitudinal and transverse displacements of the bottom face, as well as zero longitudinal displacement and the given deflection w_f of the upper face. The transformed Lamé equations produce the following relation between the images of the face deflection and normal stress at the interface [13]

$$\sigma_{if}^{F(H)}(\omega,t) = E_1 \omega F(\omega h_c) w_f^{F(H)}(\omega,t), \quad (3)$$

where

$$F(\omega h_c) = \frac{\cosh(\omega h_c)\sinh(\omega h_c) + \psi\omega h_c}{\sinh^2(\omega h_c) - (\psi\omega h_c)^2}.$$

Here, the reduced parameters of the core stiffness E_1 and ψ are introduced through Young's modulus, E_c, and the Poisson's ratio, v_c, of the core as

$$E_1 = 2\psi E_c/(1+v_c)^2, \quad \psi = (1+v_c)/(3-v_c)$$

for the plane stress state or as

$$E_1 = 2\psi E_c(1-v_c)/(1+v_c), \quad \psi = 1/(3-4v_c)$$

both for the plane strain and axisymmetric states.

In the case of impact, the Hertzian indentation is neglected. The equation of motion of the impactor of the mass m at the contact with the face is

$$m\frac{\partial^2 w_0(t)}{\partial t^2} = -P(t), \tag{4}$$

where $w_0(t)$ is the face deflection under the impactor, $P(t)$ is the contact force. The effect of the impactor rebound from the face sheet is not considered. The impactor is assumed "to stick" to the face sheet once the contact had onset.

3. Quasi-static solutions

3.1. Response to prescribed loading

Applying the cosine Fourier transformation to Eq. (1) and Hankel transformation to Eq. (2) with the assumption of quasi-static response ($\rho_f = 0$), the equations are reduced to

$$\begin{aligned} &D_f\omega^4 w_f^F(\omega,t) + \sigma_{if}^F(\omega,t) = P(t)/2b,\\ &D_f\omega^4 w_f^H(\omega,t) + \sigma_{if}^H(\omega,t) = P(t)/2\pi. \end{aligned} \tag{5}$$

The closed-form solutions for the originals of the face deflection and normal interfacial stress are obtained by substituting Eq. (3) into Eq. (5) and applying the inverse Fourier or Hankel transformation

$$\begin{aligned} w_f^{pl}(\xi,t) &= \frac{P(t)}{\pi E_1 b}\int_0^\infty \frac{\cos(\xi\bar\omega)\,d\bar\omega}{\bar\omega\mu(\xi\bar\omega)},\\ \sigma_{if}^{pl}(\xi,t) &= \frac{P(t)}{\pi x_n b}\int_0^\infty \frac{\cos(\xi\bar\omega)\,d\bar\omega}{\lambda(\xi\bar\omega)}, \end{aligned} \tag{6}$$

$$\begin{aligned} w_f^{ax}(\xi,t) &= \frac{P(t)}{2\pi E_1 x_n}\int_0^\infty \frac{J_0(\xi\bar\omega)\,d\bar\omega}{\mu(\xi\bar\omega)},\\ \sigma_{if}^{ax}(\xi,t) &= \frac{P(t)}{2\pi x_n^2}\int_0^\infty \frac{\bar\omega J_0(\xi\bar\omega)\,d\bar\omega}{\lambda(\xi\bar\omega)}, \end{aligned} \tag{7}$$

where

$$\mu(\xi\bar\omega) = \bar\omega^3 + F(\bar\omega/\varepsilon), \quad \lambda(\xi\bar\omega) = \frac{\mu(\xi\bar\omega)}{F(\bar\omega/\varepsilon)}$$

and J_0 is the zero-order Bessel function. The dimensionless variables $\bar\omega = \omega x_n$, $\xi = x/x_n$ ($\xi = r/x_n$) and $\bar\omega/\varepsilon = \omega h_c$ are introduced using the characteristic length $x_n = \sqrt[3]{D_f/E_1}$ and non-dimensional parameter $\varepsilon = x_n/h_c$.

The parameter ε characterizes the relationship between the bending stiffness of the face and the core layer; ε is small for the majority of real sandwich structures. The function $F(\bar\omega/\varepsilon)$ equals to unity at $\varepsilon \to 0$ that allows to derive the improper integrals analytically, e.g.

$$\sigma_{if}^{pl}(0,t) \overset{\varepsilon\to 0}{\to} \frac{2P}{3\sqrt{3}x_n b}, \quad \sigma_{if}^{ax}(0,t) \overset{\varepsilon\to 0}{\to} \frac{P}{3\sqrt{3}x_n^2}. \tag{8}$$

In a general case, the functions can be expanded in asymptotic series of ε, e.g.

$$w_f^{pl}(0,t) = \frac{P(t)}{\pi E_1 b}\left(\ln\left(\frac{1}{\varepsilon}\right) + n_1 + \varepsilon^3 n_2 + O(\varepsilon^6)\right), \tag{9}$$

$$w_f^{ax}(0,t) = \frac{P(t)}{2\pi E_1 x_n}\left(\frac{2\pi}{3\sqrt{3}} - \varepsilon n_3 + \varepsilon^4 n_4 + O(\varepsilon^7)\right). \tag{10}$$

Here, the factors n_i are functions of Poisson's ratio of the core, e.g.

$$\begin{aligned} n_1 &= \int_0^\infty \frac{(1-\Phi(\varsigma))\,d\varsigma}{(\varsigma+1)(\varsigma+\Phi(\varsigma))},\\ n_3 &= \int_0^\infty \frac{\varsigma^3\Phi(\varsigma)\,d\varsigma}{\varsigma+\Phi(\varsigma)},\\ \Phi(\varsigma) &= \varsigma(F(\varsigma)-1), \quad \varsigma = \frac{\bar\omega}{\varepsilon} \end{aligned}$$

and it is convenient to substitute them by the following approximations:

$$\begin{aligned} &n_1 = 0.5 - 0.6v_n, \quad n_2 = 0.4 + 0.2v_n,\\ &n_3 = 0.8 + 0.6v_n, \quad n_4 = 1.5 + 0.7v_n, \end{aligned}$$

where $v_n = 2v_c^3/(1+v_c)^3$ for the plane stress state and $v_n = 2v_c^3$ for the other cases.

The solution also allows to obtain the bending moment in the face with the maximum magnitude directly under the load. In the plane problem, the original and the image of the bending moment are defined as

$$M_f^{pl}(x,t) = -D_f\frac{\partial^2 w_f(x,t)}{\partial x^2} \;\to\; M_f^F(\omega,t) = D_f\omega^2 w_f^F(\omega,t)$$

so that

$$\begin{aligned} M_f^{pl}(\xi,t) &= \frac{P(t)x_n}{\pi b}\int_0^\infty \frac{\bar\omega\,d\bar\omega}{\mu(\xi\bar\omega)},\\ M_f^{pl}(0,t) &\overset{\varepsilon\to 0}{\to} \frac{2}{3\sqrt{3}}\frac{x_n}{b}. \end{aligned} \tag{11}$$

The solution for the bending moment is also available for the axisymmetric formulation. In this case, the solution has singularity of the type $\ln(\xi)$ due to assumptions of the theory of bending of thin plates and, therefore, the solution is not interesting from the practical point of view.

3.2. Response to impact

The deflection at $\xi = 0$ can be represented as

$$w_0(t) = P(t)\Psi_w \quad \rightarrow \quad w_0^{\mathrm{L}}(p) = P^{\mathrm{L}}(p)\Psi_w, \tag{12}$$

where Ψ_w is obtained from the first formulas of Eqs. (6) and (7). On the other hand, after the Laplace transformation Eq. (4) becomes

$$mp^2 w_0^{\mathrm{L}}(p) = -P^{\mathrm{L}}(p) + mv, \tag{13}$$

where v is the initial impact velocity. The image of the face deflection at the point of impact is obtained by the combination of Eqs. (12) and (13)

$$w_0^{\mathrm{L}}(p) = \frac{v}{p^2 + k^2}, \quad k^2 = \frac{1}{m\Psi_w}$$

from which the original is produced by the inverse Laplace transformation as

$$w_0(t) = \frac{v}{k}\sin(tk). \tag{14}$$

The contact force is determined by substitution of Eq. (14) into Eq. (12) as

$$P(t) = vmk\sin(tk). \tag{15}$$

4. Dynamic solutions

4.1. Response to prescribed loading

At $\rho_{\mathrm{f}} \neq 0$, the double Fourier–Laplace transformation of Eq. (1) produces

$$D_{\mathrm{f}}\omega^4 w_{\mathrm{f}}^{\mathrm{FL}}(\omega,p) + \sigma_{\mathrm{if}}^{\mathrm{F}}(\omega,p) + \rho_{\mathrm{f}}h_{\mathrm{f}}p^2 w_{\mathrm{f}}^{\mathrm{FL}}(\omega,p) = P^{\mathrm{L}}(p)/2b \tag{16}$$

and the double Hankel–Laplace transformation of Eq. (2) gives

$$D_{\mathrm{f}}\omega^4 w_{\mathrm{f}}^{\mathrm{HL}}(\omega,p) + \sigma_{\mathrm{if}}^{H}(\omega,p) + \rho_{\mathrm{f}}h_{\mathrm{f}}p^2 w_{\mathrm{f}}^{\mathrm{HL}}(\omega,p) = P^{\mathrm{L}}(p)/2\pi. \tag{17}$$

Taking into account Eq. (3), the image of the face deflection is

$$w_{\mathrm{f}}^{\mathrm{F(H)L}}(\omega,p) = \frac{1}{2\varphi}\frac{P^{\mathrm{L}}(p)}{D_{\mathrm{f}}\omega^4 + E_1\omega F(\omega h_{\mathrm{c}}) + p^2\rho_{\mathrm{f}}h_{\mathrm{f}}}, \tag{18}$$

where $\varphi = b$ or $\varphi = \pi$ for the plane or axisymmetric formulations, respectively.

The final solutions are determined by the double inverse Fourier–Laplace transform. Among possible functions $P(t)$, the fundamental force–time dependence is an impulse function $P(t) = I\delta(t)$ ($P^{\mathrm{L}}(p) = I$). In this case, the originals of the face deflection and the interfacial stress under the ($\xi = 0$) are

$$w_0^{\mathrm{pl}}(\tau) = \frac{I}{\pi bE_1 t_n}\int_0^\infty \frac{\mathrm{d}\bar{\omega}}{\eta(\bar{\omega},\tau)}, \qquad \sigma_0^{\mathrm{pl}}(\tau) = \frac{I}{\pi bt_n x_n}\int_0^\infty \frac{\bar{\omega}F(\bar{\omega}/\varepsilon)\,\mathrm{d}\bar{\omega}}{\eta(\bar{\omega},\tau)} \tag{19}$$

in the plane formulation and

$$w_0^{\mathrm{ax}}(\tau) = \frac{I}{2\pi E_1 t_n x_n}\int_0^\infty \frac{\bar{\omega}\mathrm{d}\bar{\omega}}{\eta(\bar{\omega},\tau)}, \qquad \sigma_0^{\mathrm{ax}}(\tau) = \frac{I}{2\pi t_n x_n^2}\int_0^\infty \frac{\bar{\omega}^2 F(\bar{\omega}/\varepsilon)\,\mathrm{d}\bar{\omega}}{\eta(\bar{\omega},\tau)} \tag{20}$$

in the axisymmetric formulation. The function $\eta(\bar{\omega},\tau)$ and dimensionless time τ are introduced using the characteristic time t_n,

$$\eta(\bar{\omega},\tau) = \frac{\sqrt{\bar{\omega}^4 + \bar{\omega}F(\bar{\omega}/\varepsilon)}}{\sin(\tau\sqrt{\bar{\omega}^4 + \bar{\omega}F(\bar{\omega}/\varepsilon)})}, \qquad \tau = \frac{t}{t_n}, \quad t_n = \sqrt{\frac{\rho_{\mathrm{f}}h_{\mathrm{f}}x_n}{E_1}}.$$

The structural response to the impulse $I = 1$ N s is illustrated in Figs. 2 and 3. The response to an arbitrary function $P(t)$ can be derived using Duhamel's integral, i.e. through convolution of this function with Eqs. (19) or (20), e.g.

$$w_0^{\mathrm{pl}}(\tau) = \frac{I}{\pi bE_1 t_n}\int_0^\tau\int_0^\infty \frac{P(\tau-\tau_1)}{\eta(\bar{\omega},\tau_1)}\,\mathrm{d}\bar{\omega}\,\mathrm{d}\tau_1. \tag{21}$$

4.2. Response to impact

Using dimensionless Laplace transformation variable $\bar{p} = pt_n$, which corresponds to the dimensionless time τ, the combined solution of Eqs. (18) and (13) produces the following images of the face deflection, interfacial stress and contact force at $\xi = 0$,

$$w_0^{\mathrm{L}}(\bar{p}) = \frac{vt_n}{\bar{p}^2 + \gamma^2/f_1}, \qquad \sigma_0^{\mathrm{L}}(\bar{p}) = \frac{1}{x_n}\frac{g_1E_1vt_n}{\bar{p}^2f_1 + \gamma^2}, \qquad P^{\mathrm{L}}(\bar{p}) = \frac{1}{t_n}\frac{mv\gamma^2}{\bar{p}^2f_1 + \gamma^2} \tag{22}$$

in the plane formulation, and

$$w_0^{\mathrm{L}}(\bar{p}) = \frac{vt_n}{\bar{p}^2 + \gamma^2/f_2}, \qquad \sigma_0^{\mathrm{L}}(\bar{p}) = \frac{1}{x_n}\frac{g_2E_1vt_n}{\bar{p}^2f_2 + \gamma^2}, \qquad P^{\mathrm{L}}(\bar{p}) = \frac{1}{t_n}\frac{mv\gamma^2}{\bar{p}^2f_2 + \gamma^2} \tag{23}$$

in the asymmetric formulation, where

$$\gamma^2 = \begin{cases} \rho_{\mathrm{f}}h_{\mathrm{f}}x_n b/m & \text{in the plane formulation,} \\ 2\rho_{\mathrm{f}}h_{\mathrm{f}}x_n^2/m & \text{in the axisymmetric formulation.} \end{cases}$$

The non-dimensional parameter γ relates the face mass in the deformed zone to the impactor mass m and characterizes the type of the impact. If this parameter is small, the influence of the face inertia on the structural response is negligible, and the response is close to the

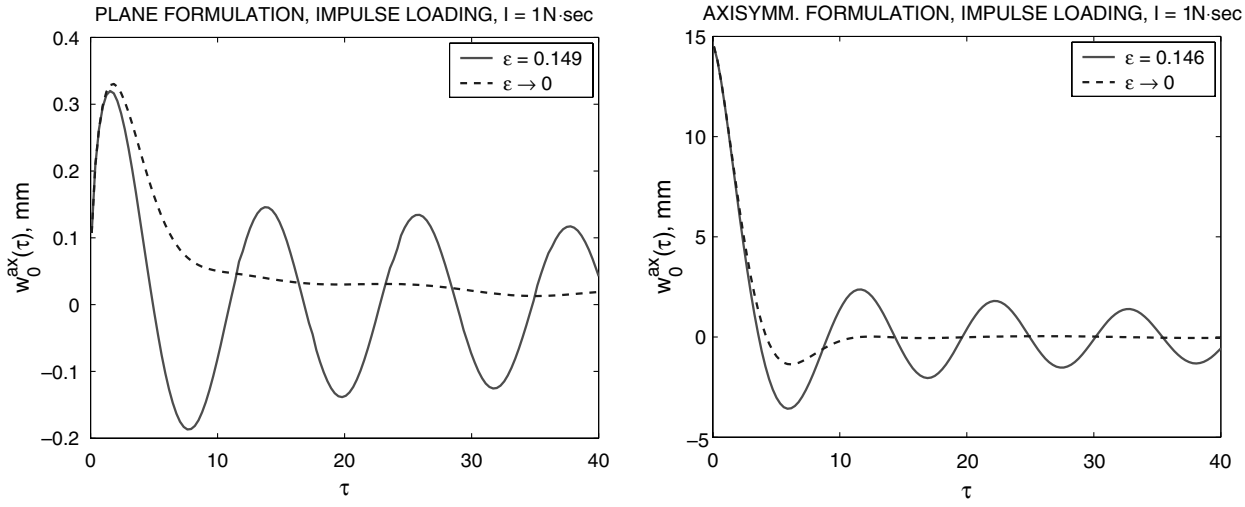

Fig. 2. Maximum face deflection vs. dimensionless time.

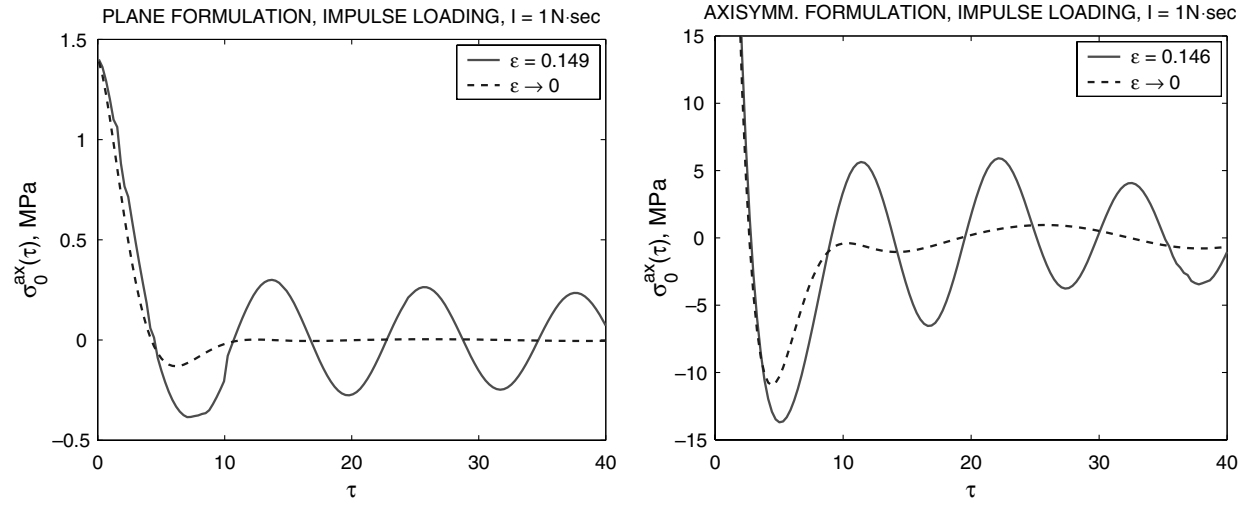

Fig. 3. Maximum normal stress at the interface vs. dimensionless time.

quasi-static case. For large values of γ the quasi-static approach is invalid.

In Eqs. (22) and (23), the following auxiliary functions are introduced:

$$f_j(\bar{p}) = \frac{1}{\pi}\int_0^\infty \frac{\bar{\omega}^{j-1}\mathrm{d}\bar{\omega}}{\bar{\omega}^4 + \bar{\omega}F(\bar{\omega}/\varepsilon) + \bar{p}^2},$$
$$g_j(\bar{p}) = \frac{1}{\pi}\int_0^\infty \frac{\bar{\omega}^{j}F(\bar{\omega}/\varepsilon)\,\mathrm{d}\bar{\omega}}{\bar{\omega}^4 + \bar{\omega}F(\bar{\omega}/\varepsilon) + \bar{p}^2}, \tag{24}$$

where $j = 1, 2$.

The direct analytical inversion of Eqs. (22) and (23) is impossible. However, two efficient techniques can be used for an approximate inversion with an arbitrary small error. The first technique is based on expansion of the functions $f_j(\bar{p})$ and $g_j(\bar{p})$ from Eq. (24) in asymptotic power series of $1/\bar{p}$ at large $\bar{p}$ (i.e. at small τ). The most interesting and simple results concern the case when $\varepsilon \to 0$. In this case, the functions (24) can be evaluated as

$$g_j(\bar{p}) = f_{j+1}(\bar{p}) = \frac{1}{\bar{p}^{(3-j)/2}}\sum_{i=1}^{\infty}\frac{(-1)^{i-1}a_{j+1,i-1}}{\bar{p}^{3(i-1)/2}}, \tag{25}$$

where

$$a_{j+1,i-1} = \frac{\Gamma((i+j)/4)\Gamma((3i-j)/4)}{4\pi\Gamma(i+j)}$$

and Γ is the gamma-function. The transition of Eqs. (22) and (23) to the originals is also performed using the series. For instance, substituting Eq. (25) into the image of the contact force given by Eq. (22) produces

$$P^{\mathrm{L}}(\bar{p}) = \frac{mv\gamma^2}{a_{1,0}\bar{p}^{1/2} + \sum_{i=1}^{\infty}(-1)^i \frac{a_{1,i}}{\bar{p}^{(3i-1)/2}} + \gamma^2} \tag{26}$$

from which follows

$$P^{\mathrm{L}}(\bar{p}) = mv\gamma^2 \sum_{i=1}^{\infty} c_i(\gamma)\bar{p}^{-i/2}$$

$$\rightarrow \quad P(\tau) = \frac{mv\gamma^2}{\tau t_n} \sum_{i=1}^{\infty} c_i(\gamma) \frac{\tau^{i/2}}{\Gamma(i/2)}, \tag{27}$$

where $c_i(\gamma)$ are coefficients of expansion of the fraction from Eq. (26) in the Maclaurin series of $\bar{p}$. The face deflection w_0 and interfacial stress σ_0 are also derived by expansion in series or as the following convolutions:

$$w_0(\tau) = \frac{t_n^2}{m\gamma^2} \int_0^{\tau} P(\tau - \tau_1)\phi_1(\tau_1)\,\mathrm{d}\tau_1,$$
$$\sigma_0(\tau) = \frac{E_1 t_n^2}{m\gamma^2 x_n} \int_0^{\tau} P(\tau - \tau_1)\phi_2(\tau_1)\,\mathrm{d}\tau_1, \tag{28}$$

$$\sigma_0(\tau) = \frac{E_1 t_n^2}{m\gamma^2 x_n} \int_0^{\tau} P(\tau - \tau_1)\phi_2(\tau_1)\,\mathrm{d}\tau_1, \tag{29}$$

where

$$\phi_j(\tau) = \tau^{(2-j)/2} \sum_{i=1}^{\infty} \tau^{3i/2} \frac{(-1)^i a_{j,i}}{\Gamma((3i+4-j)/2)} \quad (j = 1, 2)$$

are originals of the functions $f_j(\bar{p})$ from Eq. (25).

The formula (27) for the force has irregularity of the type $1/\sqrt{\tau}$ for the plane formulation at $\tau \to 0$, while the deflection and stress are finite. The solutions for the axisymmetric formulation can be obtained from Eqs. (27)–(29) by replacements $\phi_1 \to \phi_2$, $\phi_2 \to \phi_3$. In this case, all the variables are finite. The structural response to the small-mass impact is illustrated in Figs. 4–6. When calculating Eqs. (27) and (28), the number of terms in the series was taken 150.

The series in Eq. (27) converge only for small and moderate values of dimensionless time τ. Such intervals of τ include maximums of the variables only for large γ. Thus, the long-duration impacts for small γ should be described by the numerical inversion of the transformations (22) and (23). For that, using the property of the Laplace transformation of a product of two functions, the images of the contact force from Eqs. (22) and (23) can be written as

$$\int_0^{\tau} P(\tau_1)(\phi_2(\tau - \tau_1) + \gamma^2(\tau - \tau_1))\,\mathrm{d}\tau_1 = \lambda(\tau),$$
$$\lambda(\tau) = \tau mv\gamma^2. \tag{30}$$

The solution of the integral equation (30) is unstable by the right part and needs a regularizing algorithm. For that, Eq. (30) has to be rewritten as

$$\int_0^T \left\{ \int_0^{\tau} P(\tau_1)H(\tau, \tau_1)\,\mathrm{d}\tau_1 - \lambda(\tau) \right\}^2 \mathrm{d}\tau + \alpha\Omega[P] \to \min, \tag{31}$$

where T is calculation time, α is a small regularizing parameter and

$$H(\tau, \tau_1) = \begin{cases} \phi_2(\tau - \tau_1) + \gamma^2(\tau - \tau_1), & \in \tau_1 < \tau, \\ 0, & \in \tau_1 > \tau. \end{cases}$$

The function $\Omega[P]$ is the Tikhonov regulizator of the second order

$$\Omega[P] = \int_0^T \left(P^2(\tau) + \left(\frac{\partial P(\tau)}{\partial \tau} \right)^2 \right) \mathrm{d}\tau.$$

Eq. (31) is well-behaved variational formulation for Eq. (30), and its solution is stable. Therefore, the required regularized solution for $P(\tau)$ minimizing the functional (31) is the solution of the following equation:

$$\int_0^T K(\tau_1, \tau)P(\tau)\,\mathrm{d}\tau + \alpha\left(P(\tau_1) - \frac{\partial^2 P(\tau_1)}{\partial \tau_1^2} \right) = F(\tau_1), \tag{32}$$

where

$$K(\tau_1, \tau) = \int_{\max(\tau_1, \tau)}^{T} H(\tilde{\tau}, \tau_1)H(\tilde{\tau}, \tau)\,\mathrm{d}\tilde{\tau},$$
$$F(\tau_1) = \int_{\tau_1}^{T} \lambda(\tau)H(\tau, \tau_1)\,\mathrm{d}\tau.$$

The Euler integro-differential equation (32) can be easily solved numerically using the method of finite differences. The structural response to the large-mass impact is illustrated in Figs. 7–9. When solving discrete analogue of Eq. (32), the step-interval of the dimensionless time was taken 0.2.

5. Quasi-static indentation tests

Experimental validation of the analytical model was carried out for two sandwich configurations. These configurations were manufactured with GFRP face sheets and two core materials; Rohacell WF51 and Divinycell H130 rigid closed-cell foams. The mechanical properties of the face sheets and foam cores were experimentally measured according to the ASTM methods. The values of Poisson's ratio were estimated by the laminate theory for the faces laminates or taken from the core manufacturers data sheets [21,22]. The mechanical properties of the materials are summarized in Table 1.

Quasi-static indentation tests were conducted on sandwich beams and panels. The size of specimens was 280×50 mm (beams) or 250×180 mm (panels). The specimens were free supported by a stiff substrate. The

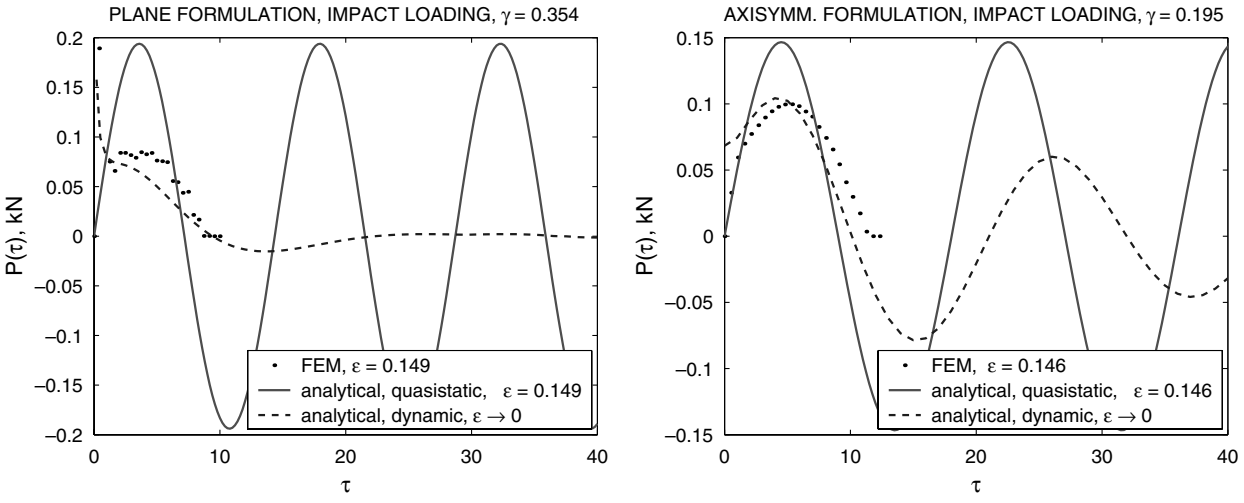

Fig. 4. Contact force vs. dimensionless time.

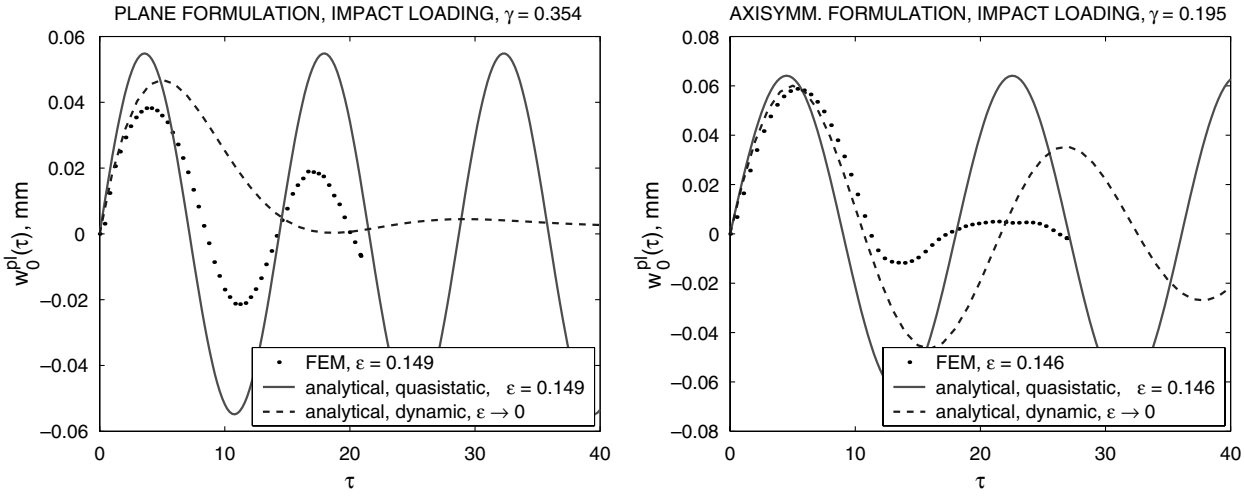

Fig. 5. Maximum face deflection vs. dimensionless time.

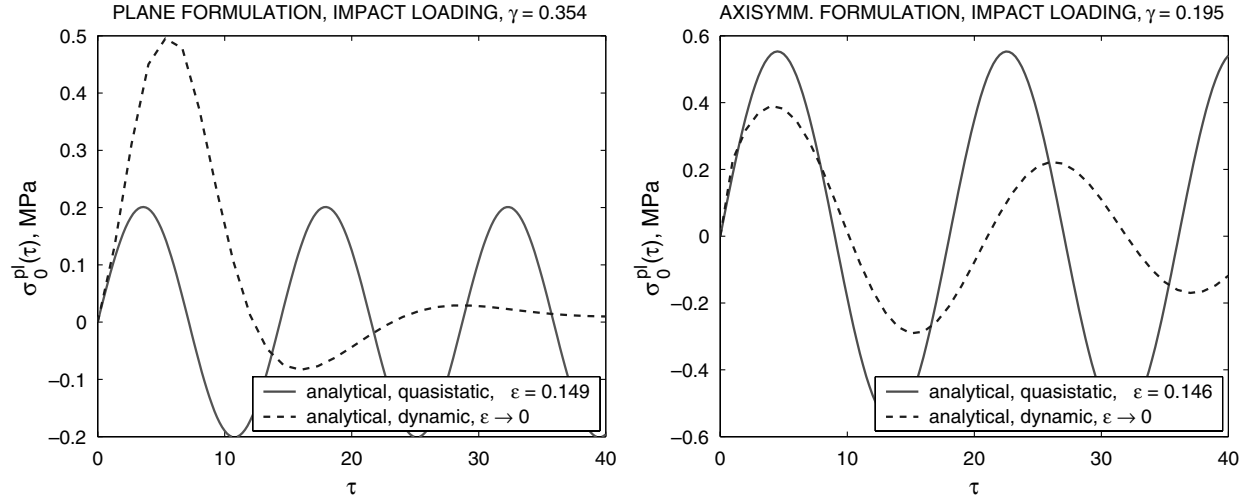

Fig. 6. Maximum normal stress at the interface vs. dimensionless time.

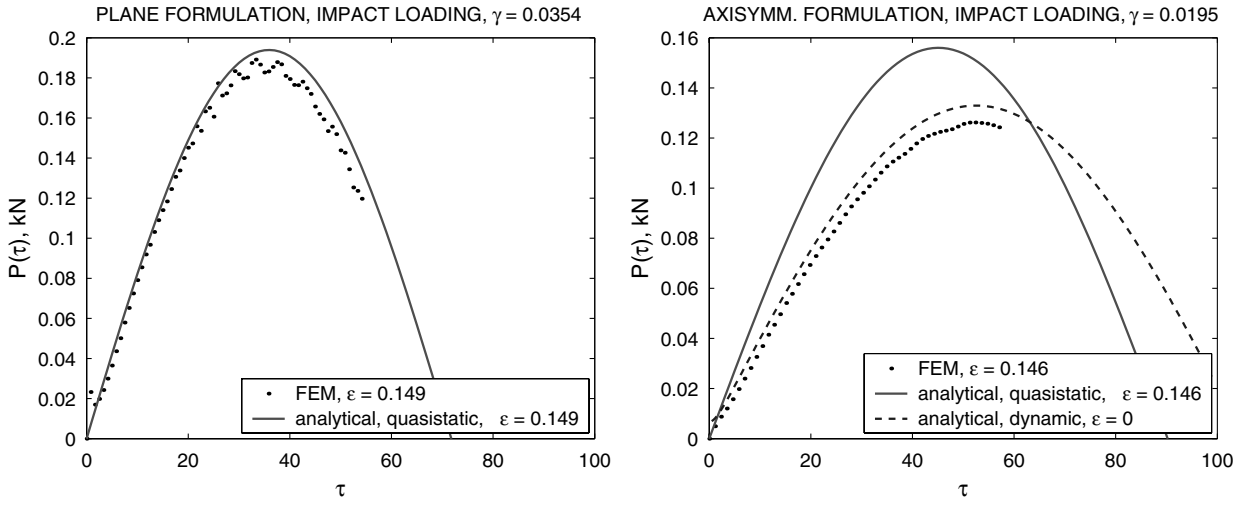

Fig. 7. Contact force vs. dimensionless time.

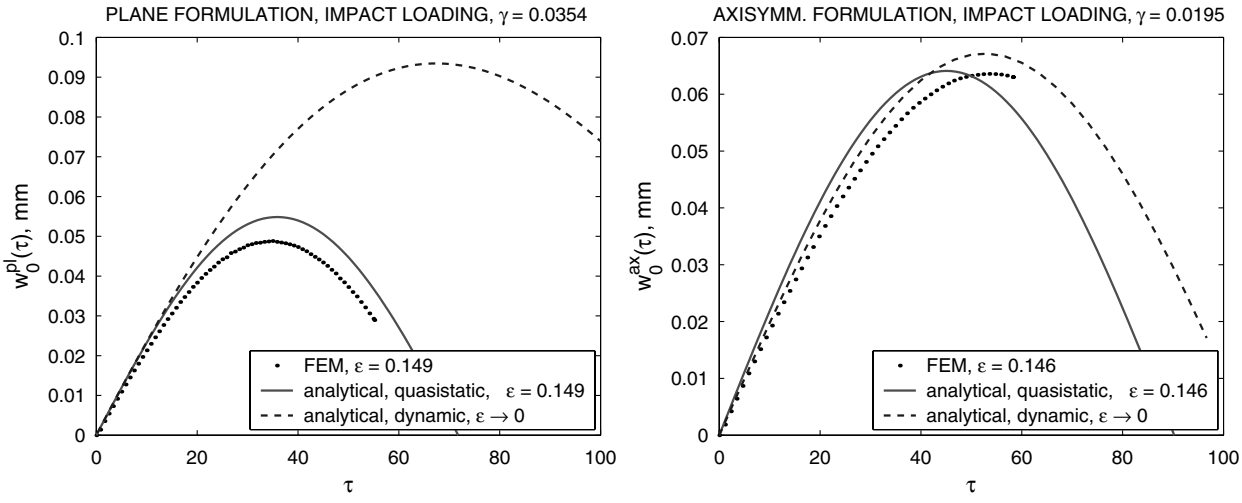

Fig. 8. Maximum face deflection vs. dimensionless time.

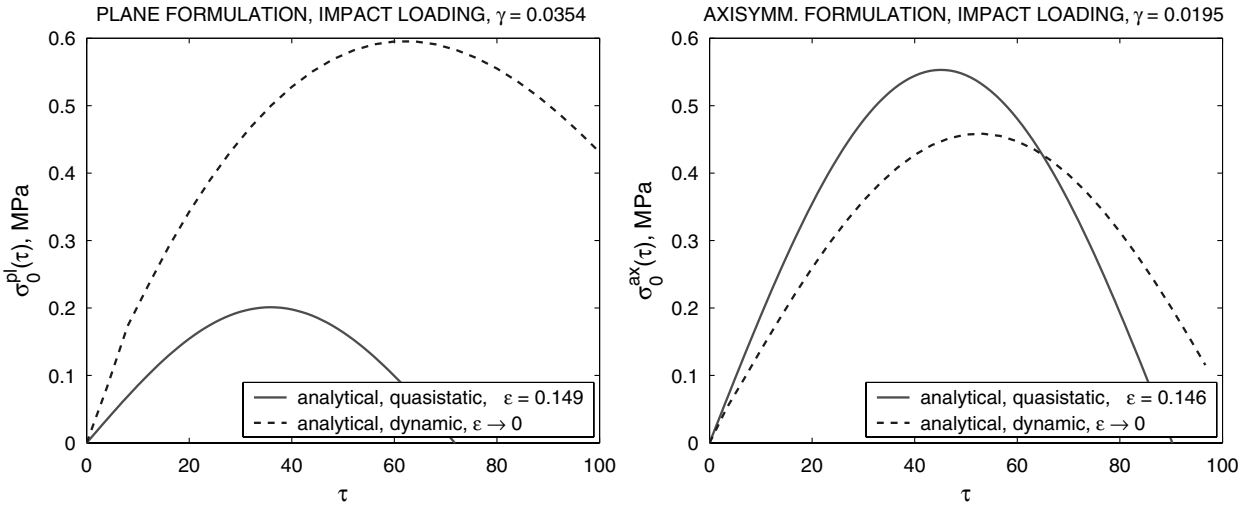

Fig. 9. Maximum normal stress at the interface vs. dimensionless time.

Table 1
Mechanical properties of the sandwich constituents

Configuration	Material	Thickness (mm)	Young's modulus (MPa)	Poisson's ratio	Density (kg/m^3)	Yield stress (MPa)
1	WF51	50	85[a]	0.42[a]	52	0.9[a]
	GFRP	2.4	16500[b]	0.25[b]	1500	–
2	H130	40	135[a]	0.32[a]	124	2.3[a]
	GFRP	1.6	15800[b]	0.25[b]	1700	–

[a] Out-plane compression.
[b] In-plane tension.

load was applied through a steel cylindrical or spherical indenter with diameter of 25 mm as shown in Fig. 1. The tests were conducted in an Instron universal testing machine under displacement control at loading rate of 2 mm/min.

6. Finite element model of impact loading

The numerical modelling of the elastic response of a sandwich structure to impact was performed using the Finite Element (FE) code *LS-DYNA*®. The analysis has been performed for the sandwich configuration 1, see Table 1.

The face sheet was meshed using 4-node shell elements. In total, 150 and 450 elements were used for modelling the face sheet in plane and axisymmetric problems, respectively. The FE mesh was condensed towards the contact area between the impactor and the face sheet; the condensation factor was 2. The core was meshed using 8-node volume elements. Fifteen elements were used through the thickness of the core. All degrees of freedom were constrained at the lower boundary of the core layer.

The impactor was modelled as a rigid body meshed using 8-node volume elements. All degrees of freedom for the impactor were constrained, except for translation in the direction normal to the plate. The contact area between the impactor and the face sheet was computed automatically by the FE code.

7. Results and discussion

If it is not indicated specially, the calculations were performed for the sandwich configuration 1, see Table 1. Some calculations relate to the case of $\varepsilon \to 0$.

7.1. Case of forced excitation

7.1.1. Static loading

The transversal stiffness of the tested sandwich panels, see Table 1, was analytically estimated using exact solutions (6) and (7) and approximate solutions (9) and (10) taking only the first term in series. The results of calculations are shown in Table 2 in comparison with the test data.

The results by analytical solutions are found to be close to the test data. The exact analytical solutions (6) and (7) produce non-conservative estimates of the contact stiffness by the maximum 20%.

7.1.2. Impulse loading

The response to the impulse, given by Eqs. (19) and (20), is illustrated in Figs. 2 and 3. The features of Eqs. (19) and (20) are that the stress in the plane formulation and the deflection in the axisymmetric formulation are finite, and the stress in the axisymmetric formulation is singular at $\tau = 0$, see Figs. 2 and 3.

The solutions presented in Figs. 2 and 3 also demonstrate the strong effect of the core thickness on the oscillation frequencies. Thus, the amplitude and frequency increase with decreasing of the core thickness, while almost no oscillations are observed for the infinite core thickness.

7.2. Case of impact loading

Two different impact cases were calculated analytically and using FE analysis; a large mass/long time impact and a small mass/short time impact. The quasi-static solutions were implemented through Eqs. (6), (7), (14) and (15). The dynamic solutions were obtained using Eqs. (27)–(29) for small mass/short time impact or

Table 2
Transversal stiffness, P/w_0 (N/mm)

Configuration	Plane problem			Axisymm. problem		
	Test[a]	Eq. (6)	Eq. (9)	Test[a]	Eq. (7)	Eq. (10)
1	3.01	3.32	3.59	2.25	2.43	1.99
2	4.36	4.50	4.95	1.89	1.95	1.74

[a] Mean value.

using Eqs. (28), (29) and (32) for large mass/long time impact.

7.2.1. Small mass/short time impact case; $m = 0.01$ kg, $v = 1$ m/s

Figs. 4–6 demonstrate the response of the sandwich structure to the small mass/short time impact. In general, the quasi-static solutions produce conservative estimation for the face deflection, interfacial stress and contact force, especially in the plane formulation. This demonstrates important role of the face inertia under impact by a small mass.

The maximums of analytical dynamic solutions and FE analysis are found in good agreement. The dynamic solutions demonstrates fast dissipation of the impact energy due to non-stationary oscillations of the face sheet. In the FE analysis, the oscillations are damped even faster due to the impactor rebound. In general, the FE analysis confirms the singular property of Eq. (27) for the plane formulation where the contact force has irregularity $1/\sqrt{\tau}$ at $\tau \to 0$.

7.2.2. Large mass/long time impact; $m = 1$ kg, $v = 0.1$ m/s

Figs. 7–9 illustrate the response of the sandwich structure to the large mass/long time impact. The dynamic analytical solution for the contact force was not obtained in the plane formulation due to singularity of Eq. (32). The quasi-static solutions produce good estimation of the contact force and deflection and are in good agreement with the FE calculations. Thus, the face inertia can be neglected when considering the impact by a large mass.

In the plane formulation, the dynamic solution produces non-conservative results in comparison with quasi-static approach and FE analysis. This fact can be explained by underestimating the transversal stiffness due to the assumption $\varepsilon = 0$ and may be overcome by accounting for the finite core thickness when expansioning the functions (24) into power series. In the axisymmetric formulation, all the solutions are in good agreement with each other, because the underestimating of the core stiffness is of the smaller importance.

8. Conclusions

The presented analytical solutions deal with the elastic response of sandwich beams and panels to local forced excitation or impact by a rigid body. The solutions concern the plane and axisymmetric formulations. The main results of this study can be outlined as

- The closed-form solutions were obtained for case of forced excitation, including the face deflection and interface stress. Explicit formulas were derived for an impulse loading. The quasi-static solutions were verified with experiments showing good agreement;
- Problem of non-stationary oscillations excited by impact was solved. It was shown that the quasi-static solutions are sufficient for the case of a large mass/long time impact, while the face inertia cannot be neglected under a small mass/short time impact. In general, the analytical results were obtained in good agreement with FE analysis;
- The presented solutions can be further used for prediction of failure onset in foam-cored sandwich structures subject to local loads.

Acknowledgements

Vitaly Koissin wishes to thank the Swedish Institute for financial support. Andrey Shipsha wishes to thank the Office of Naval Research for financial support through the program officer Dr. Y.S. Rajapakse. Some sandwich panels for experimental study were kindly provided by Dr. Per Wennhage (Department of Aeronautical and Vehicle Engineering, KTH, Sweden).

References

[1] Shipsha A, Hallström S, Zenkert D. Failure mechanisms and modelling of impact damage in sandwich beams—A 2D approach: Part I—Experimental investigation. J Sandwich Struct Mater 2003;5(1):7–32.
[2] Lolive É, Berthelot J-M. Non-linear behaviour of foam cores and sandwich materials, Part II: Indentation and three-point bending. J Sandwich Struct Mater 2002;4(4):297–352.
[3] Thomsen OT. Analysis of local bending effects in sandwich plates with orthotropic face layers subjected to localised loads. J Compos Struct 1993;25:511–20.
[4] Thomsen OT. Theoretical and experimental investigation of local bending effects in sandwich plates. J Compos Struct 1995;30:85–101.
[5] Hetényi MI. Beams on elastic foundation. Ann Arbor: University of Michigan Press; 1946.
[6] Zenkert D. An introduction to sandwich construction. London: Chameleon Press; 1995.
[7] Kármán T, Biot MA. Mathematical methods in engineering. New York: McGraw-Hill; 1940.
[8] Slepian LI. Nonstationary elastic waves. Leningrad: Sudostroenie; 1972 [in Russian].
[9] Olsson R. Engineering method for prediction of impact response and damage in sandwich panels. J Sandwich Struct Mater 2002;4(1):3–29.
[10] Pasternak PL. Fundamentals of a new method of analyzing structures on an elastic foundation by means of two foundation moduli. Moscow–Leningrad: Stroigiz; 1954 [in Russian].
[11] Ilgamov MA. Analysis of shells with elastic core. Moscow: Nauka; 1987 [in Russian].
[12] Skvortsov VR. Boundary effects and local stability of sandwich panels. In: Proceedings of the Euromech 360 Colloquium, Saint-Etienne, 1997, p. 175–82.
[13] Skvortsov VR. Exact analysis of sandwich plates bending based on elasticity theory and the technique of integral transformations.

In: Proceedings of 5th International Conference on Mechanics of Sandwich Structures, Zurich, 2000. p. 129–40.
[14] Vlasov VZ, Leont'ev NN. Beams, plates and shells on elastic foundations. Moscow: 1960 [in Russian, English translation by IPST, Jerusalem, 1966].
[15] Allen HG. Analysis and design of structural sandwich panels. Oxford: Pergamon Press; 1969.
[16] Biot MA. Bending of an infinite plate on an elastic foundation. J Appl Mech 1937;4(1):A1–7.
[17] Timoshenko SP, Woinowsky-Krieger S. Theory of plates and shells. New York: McGraw-Hill; 1959.
[18] Sneddon IN. Fourier transforms. In: International Series in Pure and Applied Mathematics. New York: McGraw-Hill; 1951.
[19] Ufliand YaS. Integral transformations in the theory of elasticity. Leningrad: Nauka; 1972 [in Russian].
[20] Sorokin SV et al. The active control of vibrations of composite beams by parametric stiffness modulation. Eur J Mech A/Solids 2000;19:873–90.
[21] DIVINYCELL. Technical Manual H–Grade. Laholm: Divinycell Int. AB, 1995.
[22] ROHACELL. Technical Manual. Darmstadt: Röhm GmbH, 1987.